AFRL-RX-WP-JA-2015-0183

CONTROL OF ANION IN CORPORATION IN THE MOLECULAR BEAM EPITAXY OF TERNARY ANTIMONIDE SUPERLATTICES FOR VERY LONG WAVELENGTH INFRARED DETECTION (POSTPRINT)

H. J. Haugan, G. J. Brown, and L. Grazulis
AFRL/RXAN

S. Elhamri
University of Dayton

OCTOBER 2015
Interim Report

AIR FORCE RESEARCH LABORATORY
MATERIALS AND MANUFACTURING DIRECTORATE
WRIGHT-PATTERSON AIR FORCE BASE, OH 45433-7750
AIR FORCE MATERIEL COMMAND
UNITED STATES AIR FORCE

NOTICE AND SIGNATURE PAGE

Using Government drawings, specifications, or other data included in this document for any purpose other than Government procurement does not in any way obligate the U.S. Government. The fact that the Government formulated or supplied the drawings, specifications, or other data does not license the holder or any other person or corporation; or convey any rights or permission to manufacture, use, or sell any patented invention that may relate to them.

This report was cleared for public release by the USAF 88th Air Base Wing (88 ABW) Public Affairs Office (PAO) and is available to the general public, including foreign nationals.

Copies may be obtained from the Defense Technical Information Center (DTIC) (http://www.dtic.mil).

AFRL-RX-WP-JA-2015-0183 HAS BEEN REVIEWED AND IS APPROVED FOR PUBLICATION IN ACCORDANCE WITH ASSIGNED DISTRIBUTION STATEMENT.

//Signature//

GAIL J. BROWN
Nanoelectronic Materials Branch
Functional Materials Division

//Signature//

DIANA M. CARLIN, Chief
Nanoelectronic Materials Branch
Functional Materials Division

//Signature//

KAREN R. OLSON, Actg Chief
Functional Materials Division
Materials and Manufacturing Directorate

This report is published in the interest of scientific and technical information exchange, and its publication does not constitute the Government's approval or disapproval of its ideas or findings.

REPORT DOCUMENTATION PAGE

Form Approved
OMB No. 074-0188

1. REPORT DATE (DD-MM-YYYY)	2. REPORT TYPE	3. DATES COVERED *(From – To)*
October 2015	Interim	17 January 2013 – 01 September 2015

4. TITLE AND SUBTITLE
CONTROL OF ANION IN CORPORATION IN THE MOLECULAR BEAM EPITAXY OF TERNARY ANTIMONIDE SUPERLATTICES FOR VERY LONG WAVELENGTH INFRARED DETECTION (POSTPRINT)

5a. CONTRACT NUMBER
FA8650-11-D-5800-0006

5b. GRANT NUMBER

5c. PROGRAM ELEMENT NUMBER
62102F

6. AUTHOR(S)
(see back)

5d. PROJECT NUMBER
4348

5e. TASK NUMBER

5f. WORK UNIT NUMBER
X0KY

7. PERFORMING ORGANIZATION NAME(S) AND ADDRESS(ES)
(see back)

8. PERFORMING ORGANIZATION REPORT NUMBER

9. SPONSORING / MONITORING AGENCY NAME(S) AND ADDRESS(ES)
Air Force Research Laboratory
Materials and Manufacturing Directorate
Wright Patterson Air Force Base, OH 45433-7750
Air Force Materiel Command
United States Air Force

10. SPONSOR/MONITOR'S ACRONYM(S)
AFRL/RXAN

11. SPONSOR/MONITOR'S REPORT NUMBER(S)
AFRL-RX-WP-JA-2015-0183

12. DISTRIBUTION / AVAILABILITY STATEMENT
Approved for public release; distribution unlimited. This report contains color.

13. SUPPLEMENTARY NOTES
PA Case Number: 88ABW-2014-2260; Clearance Date: 13 May 2014. Journal article published in Journal of Crystal Growth 425 (2015) 25–28. © 2015 Elsevier B. V. The U.S. Government is joint author of the work and has the right to use, modify, reproduce, release, perform, display or disclose the work. The final publication is available at http://dx.doi.org/10.1016/j.jcrysgro.2015.03.008.

14. ABSTRACT
Authors discuss how anion incorporation was controlled during the epitaxial growth process to develop InAs/GaInSb superlattice (SL) materials for very long wavelength infrared applications. A SL structure of 47.0Å InAs/21.5 Å $Ga_{0.75}In_{0.25}Sb$ was selected to create a very narrow band gap.Although a molecular beam epitaxy growth developed can produce a strain balanced ternary SL structure with a precisely controlled band gap around 50 meV, the material quality of grown SL layers is particularly sensitive to growth defects formed during an anion incorporation process. Since Group III antisites are the dominant structural defects responsible for the low radiative efficiencies, the authors focus on stabilizing III/V incorporation during SL layer growth by manipulating the growth surface condition for a specific anion crackingcondition. The optimized ternary SL materials produced an overall strong photoresponse signal with a relatively sharp band edges and a high mobility of ~10,000 cm^2/V s that is important for developing infrared materials.

15. SUBJECT TERMS
superlattices, molecular beam epitaxy, antimonides, infrared detector

16. SECURITY CLASSIFICATION OF:			17. LIMITATION OF ABSTRACT	18. NUMBER OF PAGES	19a. NAME OF RESPONSIBLE PERSON *(Monitor)*
a. REPORT	b. ABSTRACT	c. THIS PAGE			Gail J. Brown
Unclassified	Unclassified	Unclassified	SAR	8	19b. TELEPHONE NUBER *(include area code)* (937) 255-9854

Standard Form 298 (Rev. 2-89)
Prescribed by ANSI Std. Z39-18

REPORT DOCUMENTATION PAGE Cont'd

6. AUTHOR(S)

H. J. Haugan, G. J. Brown, and L. Grazulis - Materials and Manufacturing Directorate, Air Force Research Laboratory
S. Elhamri - Department of Physics, University of Dayton

7. PERFORMING ORGANIZATION NAME(S) AND ADDRESS(ES)

AFRL/RXAN
Air Force Research Laboratory
Materials and Manufacturing Directorate
Wright-Patterson Air Force Base, OH 45433-7750

University of Dayton Research Institute
Department of Physics
Dayton, Ohio 45469

Journal of Crystal Growth 425 (2015) 25–28

Contents lists available at ScienceDirect

Journal of Crystal Growth

journal homepage: www.elsevier.com/locate/jcrysgro

Control of anion incorporation in the molecular beam epitaxy of ternary antimonide superlattices for very long wavelength infrared detection

H.J. Haugan [a,*], G.J. Brown [a], S. Elhamri [b], L. Grazulis [a]

[a] Air Force Research Laboratory, Materials and Manufacturing Directorate, Wright-Patterson Air Force Base, Ohio 45433, United States
[b] Department of Physics, University of Dayton, Ohio 45469, United States

ARTICLE INFO

Available online 17 March 2015

Keywords:
A3. Superlattices
A3. Molecular beam epitaxy
B1. Antimonides
B3. Infrared detector

ABSTRACT

Authors discuss how anion incorporation was controlled during the epitaxial growth process to develop InAs/GaInSb superlattice (SL) materials for very long wavelength infrared applications. A SL structure of 47.0 Å InAs/21.5 Å $Ga_{0.75}In_{0.25}Sb$ was selected to create a very narrow band gap. Although a molecular beam epitaxy growth developed can produce a strain balanced ternary SL structure with a precisely controlled band gap around 50 meV, the material quality of grown SL layers is particularly sensitive to growth defects formed during an anion incorporation process. Since Group III antisites are the dominant structural defects responsible for the low radiative efficiencies, the authors focus on stabilizing III/V incorporation during SL layer growth by manipulating the growth surface condition for a specific anion cracking condition. The optimized ternary SL materials produced an overall strong photoresponse signal with a relatively sharp band edges and a high mobility of ~10,000 $cm^2/V\,s$ that is important for developing infrared materials.

1. Introduction

The InAs/GaInSb superlattice (noted as "ternary SL") system provides several distinctive theoretical advantages suitable for very long wavelength infrared (VLWIR) detection [1]. With increasing indium composition, a very narrow band gap can be achieved with a smaller period for the ternary SL system, leading to a larger absorption coefficient due to enhanced electron and hole wavefunction overlap [2]. More importantly, the strain can create a large splitting between the heavy hole and light hole bands in the ternary SLs, which reduces the hole hole Auger recombination process and increases the minority carrier lifetime, thus improving the device detectivity. Based on minimizing the Auger recombination, Grein et. al. [3] proposed a strain balanced VLWIR ternary SL of 47.0 Å InAs/21.5 Å $Ga_{0.75}In_{0.25}Sb$, which is the design used in our studies. Haugan et al. [4,5] have shown improvements in the quality of the ternary materials produced using molecular beam epitaxy (MBE) growth process for this design. Their optimized SL materials produced a strong photo response signal, a high mobility, and a long 300 K carrier lifetime. Although longer carrier lifetimes have been reported in mid wave InAs/InAsSb (noted as "Ga free) SLs [6], unfortunately to strain balance these Ga free SLs in a VLWIR design requires a much wider period, ~147 Å [7] versus the 68.5 Å used in this study, significantly impacting the absorption coefficient. Therefore, the ternary SL materials are still important for VLWIR detection.

In this work, using a combination of high resolution X ray diffraction (HRXRD), atomic force microscopy (AFM), temperature dependent Hall (TdH) effect, and photoconductivity measure ments, we continuously refined the MBE process and tuned growth conditions to produce high quality ternary SL materials to be used for VLWIR detection. Since most MBE grown III V heterostructures are affected by a large number of growth defects generated during the III V surface reconstruction process, we optimized the III/V stoichiometry by manipulating the growth surface condition such as anion fluxes, Sb cracking condition, and growth temperature. We used a SL structure of 47.0 Å InAs/21.5 Å $Ga_{0.75}In_{0.25}Sb$ to create the band gap around 50 meV.

2. Ternary superlattice growths

The InAs/GaInSb SL materials in this study were grown in a Varian MBE reactor equipped with dual filament effusion cells for the Group III elements, and valved cracker cells for the Group V elements. The repeated SL stacks (0.5 μm thick) and the undoped

* Corresponding author.
E-mail address: heather.haugan.ctr@us.af.mil (H.J. Haugan).

http://dx.doi.org/10.1016/j.jcrysgro.2015.03.008
0022-0248/

GaSb buffer layer (0.5 μm thick) were deposited on GaSb (100) wafers, and several series of 47.0 Å InAs/21.5 Å $Ga_{0.75}In_{0.25}Sb$ SL samples were grown over a wide range of anion flux conditions to preset the growth rates of Group III elements and the V/III flux ratio. To grow the intended ternary structure under minimum cross contamination environment of the anion fluxes, the V/III beam equivalent pressure (BEP) ratio was set at ~3 for both GaInSb and InAs layer depositions and the growth rates of 1.6 and 0.3 Å/s were used for GaInSb and InAs layers, respectively. The Sb cracking zone temperature was varied between 850 and 1000 °C in order to investigate the III Sb incorporation during a growth, while the As cracking zone temperature was set at 900 °C. Fig. 1 shows a typical strain balanced ternary structure with an excellent crystal line quality that can be achieved by using the shutter sequence described in the inset of Fig. 1. With measured period of 68.0 Å, the grown structure produced a band gap of 53 meV, or a corresponding onset wavelength of 23 μm, as demonstrated in the photoresponse (PR) spectrum in Fig. 2.

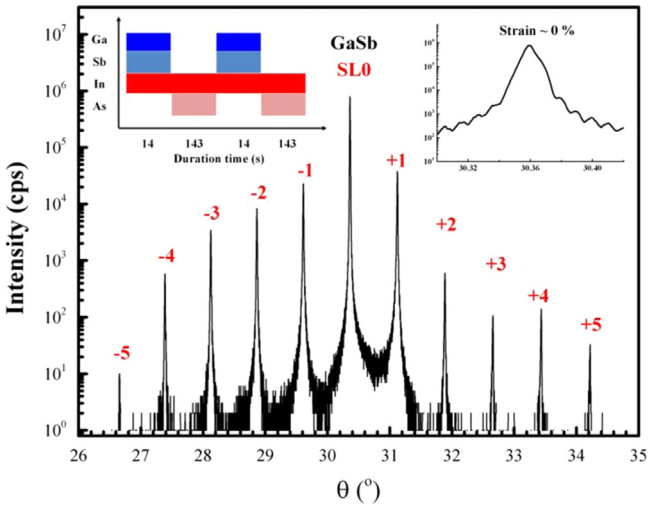

Fig. 1. X-ray diffraction patterns of a 68.0 Å period superlattice (SL) sample containing a 0.5 μm thick 47.0 Å InAs/21.5 Å $Ga_{0.75}In_{0.25}Sb$ SLs. Inset is the shutter sequence employed to create a strain-balanced ternary structure.

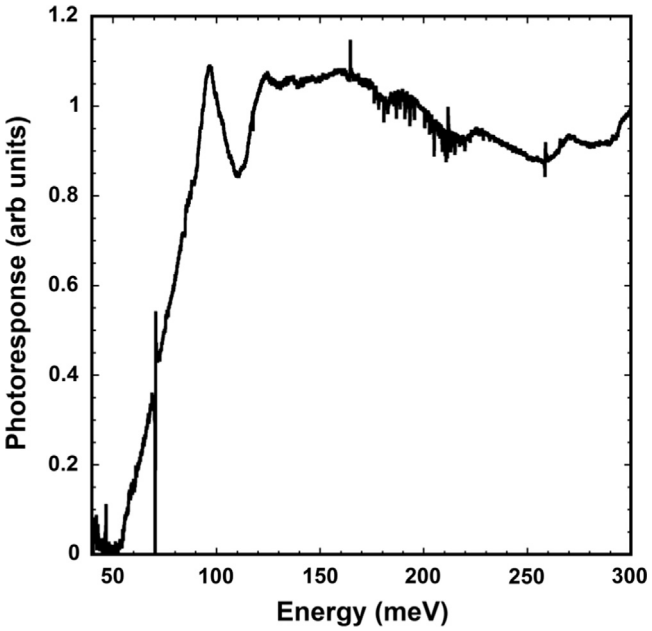

Fig. 2. Photoresponse spectrum at 10 K for the 47.0 Å InAs/21.5 Å $Ga_{0.75}In_{0.25}Sb$ superlattices.

3. Results and discussions

In order to stabilize the III Sb incorporation, a comparative deposition temperature (T_g) study was performed using various Sb cracking conditions to generate beams of tetramers, dimers, and monomers. Although some studies showed that a nearly 100% yield of Sb monomers can be achieved at a cracker temperature above ~1100 °C [8,9], no systematic study has been done to determine Sb mole fraction as a function of cracker temperature for our EPI Model 200 cc Mark V Corrosive Series Valved Cracker. Since the most obvious effect one would expect from a III/V ratio not equal to one is morphological disorder induced by the nucleation of surface defects, we used 50 μm × 50 μm area scans by AFM to monitor surface roughness as a function of the T_g. For a series of samples grown under a low Sb cracking condition (Sb cracker temperature of 850 °C), the SL roughens very quickly as the T_g is increased above 420 °C. Fig. 3 top shows the apparent surface damage observed by AFM for the sample grown at the highest T_g of 440 °C. The root mean square (RMS) value quickly changes from 2 to 61 Å as the T_g increases from 420 to 430 °C and further increases up to 80 Å at higher temperatures highlighting the noticeable surface damage that occurred at 430 °C and above. While the exact surface pitting mechanism is undetermined, it is common to see pitted surfaces in the SL layers grown under a metal rich condition due to the higher desorption rate of anion fluxes at the growth surfaces [10].

To relate the observed surface pitting phenomena to the spectral response, low temperature photoconductivity measure ments were performed and Fig. 4d plots their results. The PR spectra were collected with fourier transform infrared spectro meter over a wavelength range from 2 to 50 μm at a temperature of 10 K. Due to the relatively low resistivity of the samples, the photoconductivity was measured in the current biased mode, with a current of 0.5 mA between two parallel strip contacts on the surface. The PR intensities in Fig. 4d were measured at 100 meV above the onset. Although these intensities are given in arbitrary units (a.u.), the relative signal strengths can still be compared as the test conditions for all the samples were kept constant. The typical band gap energies of SLs grown at the same low T_g were around 48 ± 5 meV. However for $T_g > 420$ °C, the band gap did increase, as listed in Table 1. The PR intensity gradually decreases from 1.07 to 0.8 a. u. as T_g increases from 410 to 420 °C, when SL layers were grown under low Sb cracking condition generating low fraction of Sb monomers. The result of much lower PR intensity for the samples deposited at high temperatures does follow the severe surface damage trend observed in AFM scans.

Although there is a variety of ways of controlling surface roughness, such as by increasing V/III flux ratio, we increased Sb cracker temperature to generate more Sb monomers to enhance III Sb incorporation. For a series of samples grown under high Sb cracking condition (Sb cracker temperature of 950 °C), the SL layers were deposited without any noticeable surface defects at temperature as high as 470 °C. Fig. 4a plots the RMS values as a function of T_g from SL samples grown with the Sb cracker at 950 °C. In contrast to the AFM results observed in Fig. 3 top, there were no significant changes in the RMS roughness for the SL samples deposited at T_g between 410 and 450 °C, and the RMS values remained in a range of ~3 Å. Although there were no noticeable surface damages occurring at elevated temperatures (see Fig. 3 bottom), the PR signal strength was still affected by T_g. Fig. 4d indicates that the PR intensity gradually increases as T_g

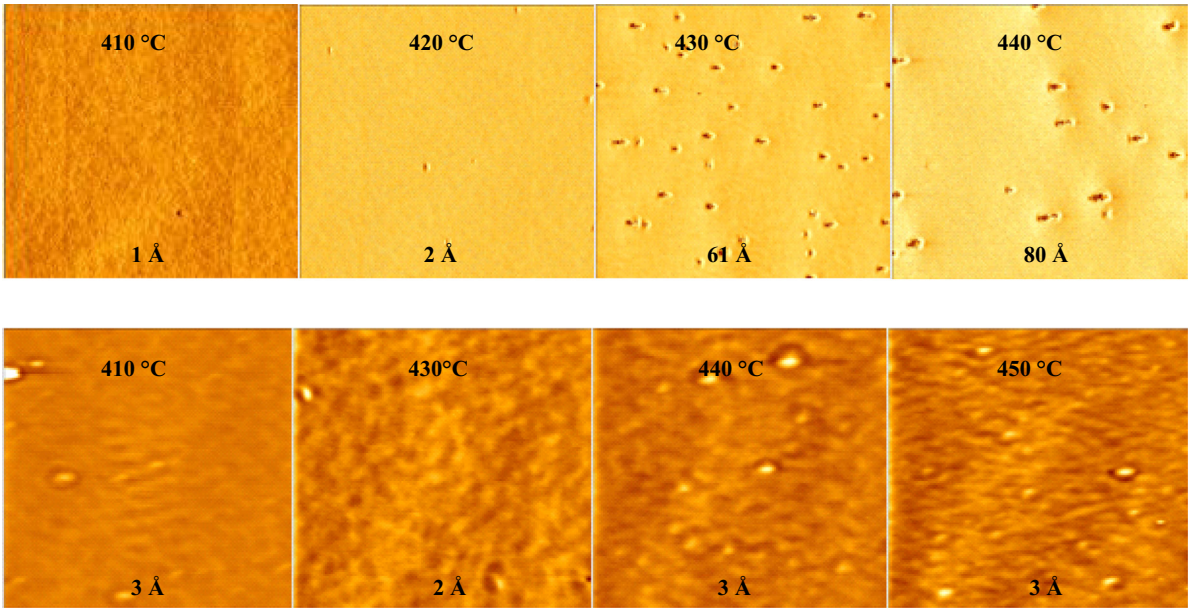

Fig. 3. AFM images of 50 μm × 50 μm area scans of 0.5 μm thick 47.0 Å InAs/21.5 Å $Ga_{0.75}In_{0.25}Sb$ superlattices grown at substrate temperature (T_s) of 410–450 °C (from left to right) performed under (top) antimony cracking temperature of 850 °C and (bottom) 950 °C, respectively. The value listed on the top (the bottom) of each image represents a T_s (an average root-mean-square roughness).

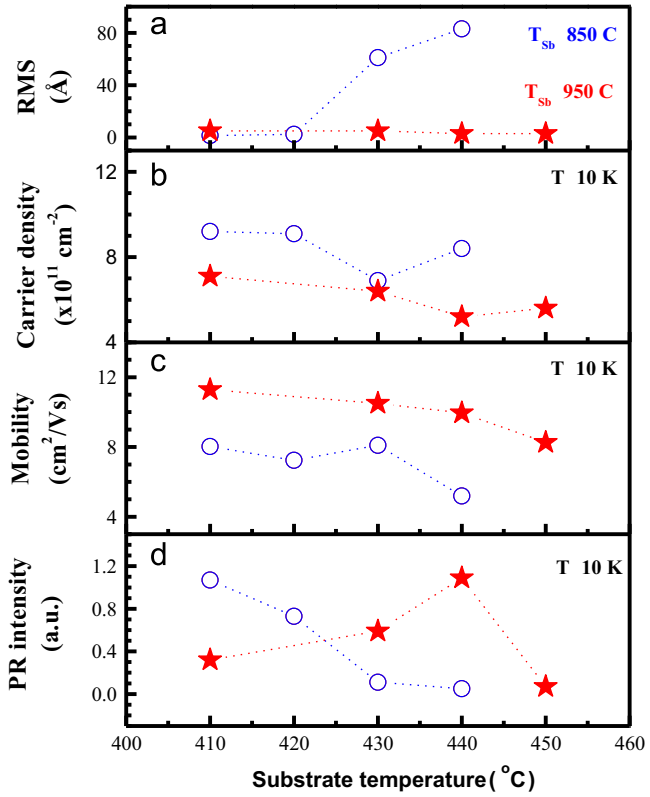

Fig. 4. (a) The root-mean-square (RMS) of 50 μm × 50 μm scans in AFM, (b) the 10 K carrier density, (c) mobility, and (d) photoresponse (PR) intensity as a function of substrate temperature for the sample series grown under antimony cracker temperature of 850 (open red circle) and 950 °C (closed blue star). For interpretation of the references to color in this figure legend, the reader is referred to the web version of this article.

increases from 410 to 440 °C, reaching a maximum at 440 °C, and then drops rapidly to less than 0.1 a.u. at 450 °C. This is in contrast to the first series, where the PR was very low at 440 °C. Evidently deposition temperature and Sb cracking condition are intimately correlated to the III Sb stoichiometry during a growth and depend directly to the quality of grown layers.

Table 1
Summary of the measurements results for the sample set. The photoresponse (PR) results are from measurements at 10 K. The cut-off wavelength λ_c is selected at the point, where the PR intensity drops by 50 %. The PR intensity was measured at 100 meV above the band gap. Antimony cracker temperature and growth temperature were noted by T_{Sb} and T_s, respectively.

Sample	T_{Sb} (°C)	T (°C)	P (Å)	E_g (meV)	λ_c (μm)
SL1	850	410	68.0	53	16.4
SL2	850	420	68.0	53	16.7
SL3	850	430	68.2	62	14.7
SL4	850	440	67.0	80	13.8
SL5	950	410	67.5	44	20.1
SL6	950	430	68.0	46	19.0
SL7	950	440	67.5	53	17.0
SL8	950	450	68.6	50	16.2

In addition to the spectral PR measurements, TdH measurements were also performed to track changes in the electrical properties under the various growth conditions. For the first series, the average sheet concentration was 8.4×10^{11} cm ^{2} at 10 K and varied by only about 1×10^{11} cm ^{2}. All of the VLWIR samples were n type. The average carrier mobility at 10 K was 7800 cm^2/V s for the first three samples but dropped to 5190 cm^2/V s at the 440 °C of T_g. While this agrees with the lowest PR result, we do not see a matching trend of degrading Hall results with increasing T_g similar to the AFM or PR intensity trends. The TdH measurements appear to be less sensitive to growth defects. The photoresponse on the other hand is very sensitive to growth defects and recombination centers. Still the Hall results do indicate when growth improvements have been made, which either decrease intrinsic carrier concentration or increase mobility, or both. For instance, for the second series of samples with the 950 °C cracker temperature, the average carrier concentration was 6.0×10^{11} cm ^{2} at 10 K, which is lower than in the first set. For the second set, the average mobility was 10,600 cm^2/V s at 10 K for

the three samples with $T_g \leq 440$ °C and the 10 K mobility dropped to 8500 cm^2/V s. In this case the Hall measurements are similar to the AFM trend of very little change in the RMS roughness but again do not track the changes in the PR.

4. Conclusions

In summary, there is a complex interplay between growth temperature, and flux condition during the MBE growth of type II ternary superlattices. This makes determining the optimum growth conditions non trivial. This report focused on the optimization of anion incorporation conditions, by manipulating anion fluxes, anion species, and growth temperature (T_g). As shown, changes in the Sb cracker temperature (T_{Sb}) selectively impact the T_g, where the photoresponse was optimized. At $T_{sb}=850$ °C, the photoresponse was the strongest at 410 °C, while at $T_{sb}=950$ °C the photoresponse was optimum at 440 °C. The inherent residual carrier concentration was slightly decreased in samples grown with the higher Sb cracker temperature and the electron mobility was higher. However, changes in the Hall and photoresponse measurements as a function of deposition conditions are very different. One of the key differences between these two experiments would be the impact of carrier recombination and lifetime on the results. The AFM results were a better indicator of the PR results. The average surface roughness of SL samples that produce a strong photoresponse was around 3 Å.

Acknowledgments

The work of H. J. Haugan was performed under Air Force contract number FA8650 11 D 5800. The authors thank S. Bower, G. Landis and A. H. Siwecki for a technical assistance with the MBE system and the sample preparation and transport the measurements, respectively.

References

[1] D.L. Smith, C. Maihiot, Rev. Mod. Phys. 62 (1990) 173.
[2] H. Kroemer, Physica E 20 (2004) 196.
[3] C.H. Grein, W.H. Lau, T.L. Harbert, M.E. Flatté, Proc. SPIE 4795 (2002) 39.
[4] H.J. Haugan, G.J. Brown, S. Elhamri, W.C. Mitchel, K. Mahalingam, M. Kim, G.T. Noe, N.E. Ogden, J. Kono, Appl. Phys. Lett. 101 (2012) 171105.
[5] Heather J. Haugan, Gail J. Brown, Krishnamurthy Mahalingam, Larry Grazulis, Gary T. Noe, Nathan E. Ogden, Junichiro Kono, J. Vac. Sci. Technol. B 32 (2014) 2C109.
[6] B.V. Olson, E.A. Shaner, J.K. Kim, J.F. Klem, S.D. Hawkins, L.M. Murray, J.P. Prineas, M.E. Flatté, T.F. Boggess, Appl. Phys. Lett. 101 (2012) 052106.
[7] A.M. Hoang, G. Chen, R. Chevallier, A. Haddadi, M. Razeghi, Appl. Phys. Lett. 104 (2014) 251105.
[8] P.D. Brewer, D.H. Chow, R.H. Miles, J. Vac. Sci. Technol. B **14** (1996) 2335.
[9] R.H. Miles, D.H. Chow, Y.H. Zhang, P.D. Brewer, R.G. Wilson, Appl. Phys. Lett. 66 (1995) 1921.
[10] B.Z. Nosho, B.R. Bennett, L.J. Whitman, M. Goldenbergen, J. Vac. Sci. Technol. B 19 (2001) 1626.